

Video alignment using unsupervised learning of local and global features

Niloufar Fakhfour^{1*}, Mohammad ShahverdiKondori² and Hoda Mohammadzade¹

^{1*}Electrical Engineering, Sharif University of Technology.

^{2*}Mathematical Sciences, Sharif University of Technology.

*Corresponding author(s). E-mail(s): niloufar.fakhfour@sharif.edu;
Contributing authors: m.shah@sharif.edu; hoda@sharif.edu;

Abstract

In this paper, we tackle the problem of video alignment, the process of matching the frames of a pair of videos containing similar actions. The main challenge in video alignment is that accurate correspondence should be established despite the differences in the execution processes and appearances between the two videos. We introduce an unsupervised method for alignment that uses global and local features of the frames. In particular, we introduce effective features for each video frame using three machine vision tools: person detection, pose estimation, and VGG network. Then, the features are processed and combined to construct a multidimensional time series that represents the video. The resulting time series are used to align videos of the same actions using a novel version of dynamic time warping named Diagonalized Dynamic Time Warping (DDTW). The main advantage of our approach is that no training is required, which makes it applicable for any new type of action without any need to collect training samples for it. For evaluation, we considered video synchronization and phase classification tasks on the Penn action dataset (Zhang et al, 2013). Also, for an effective evaluation of the video synchronization task, we present a new metric called Enclosed Area Error (EAE). The results show that our method outperforms previous state-of-the-art methods, such as TCC (Dwibedi et al, 2019), and other self-supervised and weakly supervised methods.

Keywords: Video alignment, Unsupervised, Dynamic Time Warping, Time series, Video synchronization, phase classification

1 Introduction

Many sequential processes happen daily in the world. Waking up, drinking water, and growing a plant are examples of sequential processes that are always happening. Although these processes are performed with different varieties and qualities, all the processes that show a specific action have common time points. For example, drinking a glass of water may happen at different speeds, places, and containers, but all the processes that indicate drinking water consist of 3 main steps: lifting the glass, drinking water, and lowering the glass. As a result, each process, or in other words, each action, consists of one or more phases, which are the same in terms of the order of occurrence in all similar processes (Dwibedi et al, 2019). Video alignment is a method in which the frames of the videos of two identical actions that differ in things such as scene, camera angle, and speed are matched to each other.

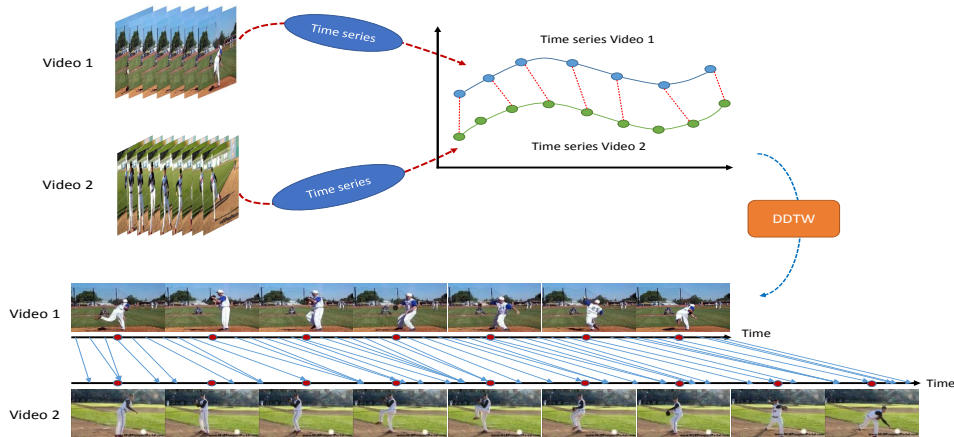


Fig. 1: We propose an unsupervised method to align pairs of videos that present the same actions. We model a video as a time series which consists of global and local features extracted from each frame. In addition, we introduce a novel DTW, called Diagonalized Dynamic Time Warping (DDTW), to find corresponding frames in each pair of videos.

The main challenge in the task of video alignment is the difference in the execution process and the appearance of the frames in videos containing the same action. For example, an action such as picking up an object from the ground can be done in various ways while recorded by the camera. This action may be done once in 5 seconds and another time in 10 seconds. The object that has risen from the ground may be a ball or a cup, big or small, red or blue. Also, the camera may record this action from the front, side, or any other angle. All these differences cause video alignment and choosing the correct method for video modeling to face many challenges.

In recent years, much research has been done in action recognition, anomaly detection, tracking, etc. However, video alignment has received less attention, while video

alignment can be used to improve all of the above. For example, in [Liu et al \(2021\)](#), novel normalized pose features invariant to video subjects’ anthropometric characteristics are introduced. The method was evaluated in the task of action recognition, and significant results were achieved. In [Li et al \(2022\)](#), the action recognition problem is considered as two separate problems: action duration misalignment and action evolution misalignment. Based on this assumption, a two-stage action alignment network is presented in this work. Video Classification ([Zhang et al, 2021](#); [Cao et al, 2020](#)) and action detection ([Fernando et al, 2017](#); [Zhao et al, 2022](#); [Song et al, 2016](#)) are other examples of the applications of video alignment that have received attention in recent years.

In the field of video alignment, self-supervised ([Dwibedi et al, 2019](#); [Purushwalkam et al, 2020](#); [Haresh et al, 2021a](#); [Liu et al, 2022](#); [Zhou and Torre, 2009](#)) and weakly-supervised methods ([Chang et al, 2019](#); [Hadji et al, 2021a](#); [Bar-Shalom et al, 2023](#); [Bojanowski et al, 2015](#)) have been presented in recent years. In some works, video alignment has been tried to solve using Dynamic Time Warping(DTW) ([Cao et al, 2020](#); [Chang et al, 2019](#); [Zhou and Torre, 2009](#)). Since DTW is not derivable and cannot be implemented using neural networks, in these works, some modified types of DTW, such as soft-dtw, which are derivable, have been used ([Cao et al, 2020](#); [Chang et al, 2019](#)). Another category of video alignment methods is based on cycle consistency loss ([Dwibedi et al, 2019](#); [Purushwalkam et al, 2020](#); [Hadji et al, 2021a](#); [Zhang et al, 2020](#)). In [Dwibedi et al \(2019\)](#), they presented a self-supervised method for learning correspondences between frames in the time domain. In this article, the network is trained based on the cycle-consistency cost function, and then the trained network is used to match the frames of a pair of videos with each other. Unlike [Dwibedi et al \(2019\)](#), [Purushwalkam et al \(2020\)](#) deals with correspondence learning in both time and space domains based on cross-cycle stability. In [Haresh et al \(2021a\)](#) and [Hadji et al \(2021a\)](#), the network is trained based on frame level and video level simultaneously. In [Haresh et al \(2021a\)](#), the network is trained based on a cost function including two terms, soft-dtw and temporal regularization. In [Hadji et al \(2021a\)](#), a weakly supervised method is presented based on a cost function consisting of dtw and cycle-consistency. In [Liu et al \(2022\)](#), another look at the subject of video alignment is given. In this work, video representation is learned to align two videos while the possibility of background frames, redundant frames, and non-monotonic frames are considered.

One of the shortcomings of the existing methods is the need to train deep networks for each class of action, which requires a lot of training samples from each action. In this work, we present an unsupervised method that can be used to align pairs of videos containing any action without any need to train a network.

The main contribution of this article is using an unsupervised approach for representing a video as a multidimensional time series representing features of its frames over time. To construct the features of a frame, we simultaneously use person detection and pose estimation algorithms to extract local features and the VGG network to extract global features. The combination of local and global features provides an effective representation of videos for accurate alignment. As shown in [Figure1](#), the

time series of videos are aligned using a modified form of DTW known as DDTW, as presented in this study.

To evaluate the effectiveness of the introduced features, we compared their performance with existing self-supervised (Misra et al, 2016; Sermanet et al, 2018; Dwibedi et al, 2019) and weakly supervised (Hadji et al, 2021a) methods in phase classification on the Penn action dataset(Zhang et al, 2013). In addition, a new evaluation metric is introduced in this work to compare the performance of alignment methods with each other.

In summary, our contributions include the following:

- Presenting an unsupervised method to align two videos.
- Modeling videos using their global and local features as well as their static and dynamic features.
- Presenting a modified DTW method for aligning time series with limited deviation.
- Presenting a new metric to compare the performance of alignment methods.

2 Method

This section describes our unsupervised method for aligning videos containing similar actions. Specifically, we model a video as a time series representing the global and local features of the video that are extracted from each frame of it. Global features are extracted by means of the VGG pre-trained network. These features show the information related to the entire frame. Local features are extracted based on pose estimation and person detection algorithms; these features are responsible for modeling changes in the subject performing the action. Figure 2 provides an illustrative overview of our proposed method for video alignment.

2.1 Feature Extraction

Features play a vital role in the areas of image processing(Kumar and Bhatia, 2014; Elharrouss et al, 2022; Chai et al, 2021) and machine vision, as extracting more valuable features leads to a better result. We use two kinds of features to model a video as a time series: global features, which are used to model the entire frame, and local features, which are used to model the details of the main subject performing the action. Features are extracted using three methods: pose estimation, person detection, and VGG network.

2.1.1 Local Features

Each action is performed by one or more main subjects. Although similar actions might differ in the scene, speed, and recording quality, the main subjects follow the same process. One important step in characterizing different actions is to represent the details of the movements of the main subject by some features. We call these features local features. Local features consist of two types: static and dynamic, which are responsible for representing the within-frame and between-frame information related to the main subject, respectively.

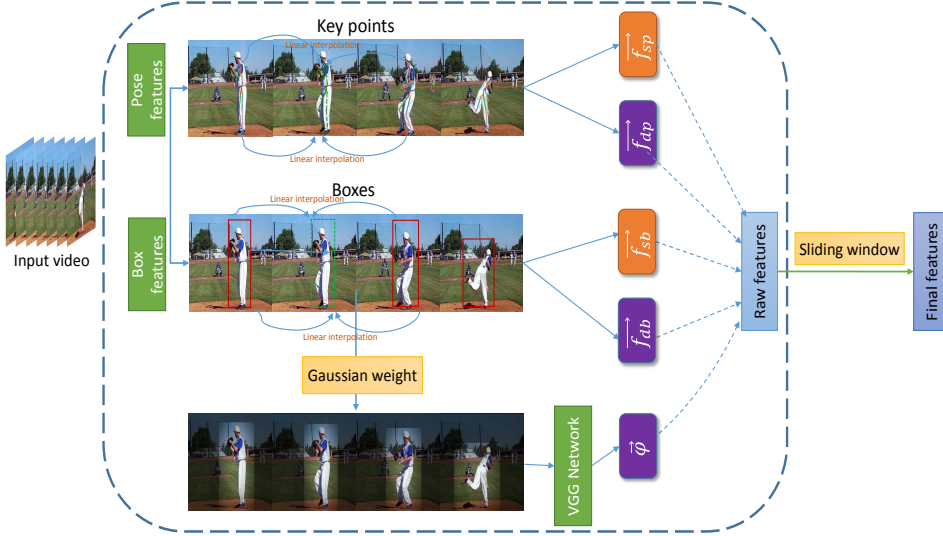


Fig. 2: In our method, two types of features are used to build time series: local features, including (pose and box features) and global features. Depending on the extracted pose and box, static and dynamic features are calculated for each image. To calculate the global features, we multiply the pixels of each frame by Gaussian weight according to the extracted box and apply the final frame to the input of the VGG network, and extract the global features based on it.

Static Features

In this work, static features refer to the features extracted from each frame independently from other frames. Static features consist of static pose features and static box features. These features represent the details of the current location of the main subject.

Static Box Features. Static box features model the main subject’s global motion and location. To extract these features, we track the main subject using the deep sort algorithm(Wojke et al, 2017) with Yolo V5(Broström, 2020) to extract the box of the main subject in each frame. After extracting the subject’s box in each frame, the length-to-width ratio and center of the boxes are used as static box features. These features explain the change in position and angle of the main subject’s body in each frame. In order to remove the effect of the initial position and the appearance characteristics of the main subject, the center of the box in the first frame is placed at the coordinate center, and the height-to-width ratio of the box is set to 1. These features in the other frames are also normalized according to the changes in the first frame:

$$f_{sb}^c(n) = c(n) - c(1) \quad \forall n \quad (1)$$

$$f_{sb}^r(n) = \frac{r(n)}{r(1)} \quad \forall n \quad (2)$$

where $c(n)$ and $r(n)$ denote the coordinates of the center and the height-to-width ratio of the subject’s box in frame n , respectively. Also, $f_{sb}^m(n)$ denotes the static box feature ($m = c$ and $m = r$ refer to the center and the height-to-width ratio of the box, respectively). Therefore, three features are extracted from each frame.

Static Pose Features. Static pose features consist of the positions of the key points of the main subject in each frame.

Human pose estimation refers to determining the position of human joints (known as body key points)(Munea et al, 2020; Babu, 2019; Chung et al, 2022). Key points extracted from pose estimation contain helpful information and details about the gestures and actions of the subject.

In this work, to extract the key points of the main subject, we use the MeTRAbs(Sáráandi et al, 2021) algorithm for pose estimation, which extracts 24 key points. After the key points are extracted, to remove the effect of the initial position of the main subject in the first frame, we shift the hip joint in the first frame to the coordinate center. We also shift all key points in all frames by the same translation vector obtained in the first frame.

$$f_{sp}^m(n) = k^m(n) - k^1(1) \quad \forall m, n \quad (3)$$

where $k^m(n)$ denotes the 2D coordinates of the m -th key point in frame n ($m = 1$ refers to the hip joint key point) and $f_{sp}^m(n)$ denotes the static pose feature corresponding to the m -th key point in frame n . Finally, 48 static pose features are extracted from each frame.

Dynamic Features

In addition to static features, to appropriately model a video of an action, some features for representing the changes between frames are also required. In this work, dynamic features refer to the features extracted based on the changes between successive frames. More specifically, these features consist of displacement vectors between the static features.

Dynamic Box Features. The displacement vector of the center position and the changes in the height-to-width ratio of the box constitute the first part of the dynamic features, which can effectively model the progression of an action. This part of dynamic features consists of the displacement vector between the static box feature in each frame and its previous frame as:

$$f_{db}^m(n) = f_{sb}^m(n) - f_{sb}^m(n - 1) \quad \forall m, n \quad (4)$$

where $f_{db}^m(n)$ denotes the dynamic pose feature in frame n . Note that $f_{db}^m(1)$ is considered to be zero. Finally, three dynamic box features are extracted for each frame.

Dynamic Pose Features. The second part of dynamic features consists of the displacement vector between the key points in each frame and its previous frame as:

$$f_{dp}^m(n) = k^m(n) - k^m(n-1) \quad \forall m, n \quad (5)$$

where $f_{dp}^m(n)$ denotes the dynamic pose feature for the m -th key point in frame n . Note that $f_{dp}^m(1)$ is considered to be zero. Finally, 48 dynamic pose features are extracted for each frame.

Interpolation for Missing Data

Each of the pose and detection algorithms may fail to extract the key points and boxes in some frames. Linear interpolation is used to estimate the missing key points and boxes using those in the most recent frames that are before and after the current frame.

2.1.2 Global Features

Our goal is to use a combination of local and global features of the frames over time to represent videos. Global features represent information over the whole frame. Obviously, an action is performed by a subject, and therefore, local features are more directly related to the type of action being performed than global features. However, the objects around the main subject, the appearance of the subject, and the background serve as important side information to represent an action.

We use VGG16 network (Simonyan and Zisserman, 2014), which is pre-trained on the Imagenet dataset (Deng et al, 2009) to extract global features. To adapt the network, we replace the fully connected layers with the 2D max-pooling layer of stride (1, 1) and filter size (7, 7), flatten layer, and the 1D max-pooling layer of stride 1 and size 8. In order to focus more on the subject than other details of the scene, a truncated 2D Gaussian weight mask is applied to the pixels of the input frame before feeding it to the network. Figure 3 illustrates the final network. The truncated 2D Gaussian weight mask is designed according to the following points:

- Pixels located inside the subject box, with a high probability, are more related to the action.
- A margin is considered for the box boundaries to reduce the error caused by the box extraction algorithm as well as not to attenuate the objects that are very close to the subject. More specifically, the height and width of the box are increased by 20 pixels¹.

The weight of the mask is constant outside of the adjusted box and is 0.2 less than the smallest weight of the 2D Gaussian on the boundaries of the box.

$$g_{x,y} = \exp\left(-\frac{(x - x_{center})^2 + (y - y_{center})^2}{2}\right) \quad (6)$$

¹Different values, including those proportional to the height of the box and other fixed values, were examined. Among these options, it was found that a value of 20 pixels yielded the best result

$$w_{x,y} = \begin{cases} g_{x,y} & p_{x,y} \in mbox \\ g_{min} - 0.2 & p_{x,y} \notin mbox \end{cases} \quad (7)$$

$w_{x,y}$ denotes the weight that should be multiplied by pixel $p(x,y)$. $mbox$ indicates the box with the margin. g_{min} represents the lowest coefficient on the boundary of the $mbox$. Finally, 64 features are extracted for each frame as global features.

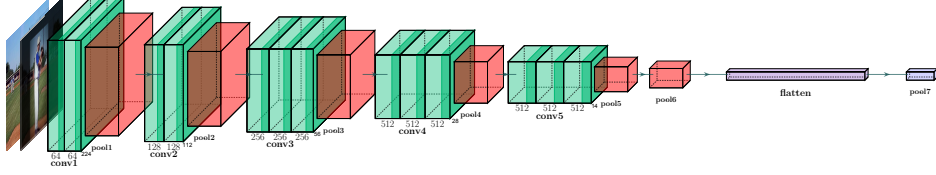


Fig. 3: VGG network is used to calculate the global features. The input of the network is a weighted frame based on the truncated 2D Gaussian weight. In order to adapt the network, the last three fully connected layers are replaced with the 2D max-pooling layer of stride (1, 1) and filter size (7, 7), followed by the flatten layer, and then the 1D max-pooling layer with a stride of 1 and a size of 8.

2.2 Construction of Time Series

After extracting the local and global feature vectors, they are concatenated, and a feature vector with a length of 166 is constructed for each frame. After that, the feature vectors of the frames of each video form a multidimensional time series that represents the video. Note that at each time step, the resulting time series has a 166 dimensional feature vector. To reduce the noise of the extracted features, a moving vector average with a window length equal to 5 is used. Also, for each time series, the mean and variance of each element of the feature vector are normalized over the time series. The final method of constructing a time series from a video is shown in Figure 2.

2.3 DDTW

Dynamic time warping(DTW)(Müller, 2007; Sakoe and Chiba, 1978) is one of the most popular algorithms for measuring the similarity between a pair of sequences and computing the best way to align them, no matter whether their lengths are equal or not. Different kinds of DTW have been developed in various fields (Wang et al, 2021; Prätzlich et al, 2016; Haresh et al, 2021b), and also some works have used DTW in video alignment tasks (Hadji et al, 2021b; Lu and Mandal, 2010). In this work, a novel method called Diagonalized Dynamic Time Warping(DDTW) is introduced, which is a generalization of the DTW method. Consider the sets $X = \{x_1, x_2, \dots, x_n\}$ and $Y = \{y_1, y_2, \dots, y_k\}$ as the frames of the first and second video, respectively, and build an $k \times n$ table D such that $D_{i,j}$ is the Euclidean distance between the feature vectors of x_i and y_j . In conventional DTW, the algorithm finds the best alignment (a path from

the down-left corner of the table to the top-right corner which can only move in three directions $\rightarrow\uparrow\nearrow$) with the minimum sum of $D_{i,j}$'s. In DDTW, a penalty coefficient is considered if the path gets further than a threshold from the diagonal. The reason for this penalty is the observation that the frames of similar actions performed by different subjects are almost linearly corresponding to each other. Therefore, the alignment path is close to the diagonal. We consider a margin m and build a new table D' as:

$$D'_{i,j} = \begin{cases} D_{i,j} & d \leq m \\ D_{i,j}(1 + \lambda(d - m)) & d > m \end{cases} \quad (8)$$

where λ is the DDTW coefficient and d is the orthogonal Euclidean distance between the table's (i, j) - cell and the diagonal. The distance d can be calculated using the formula for the distance of a point from a line in the plane; in our case, the final formula for d is the following:

$$d = \frac{|\frac{k}{n} \times i - j|}{\sqrt{\frac{k^2}{n^2} + 1}} \quad (9)$$

In the end, the best path, which has the minimum sum of the $D'_{i,j}$'s should be found. (Figure 4)

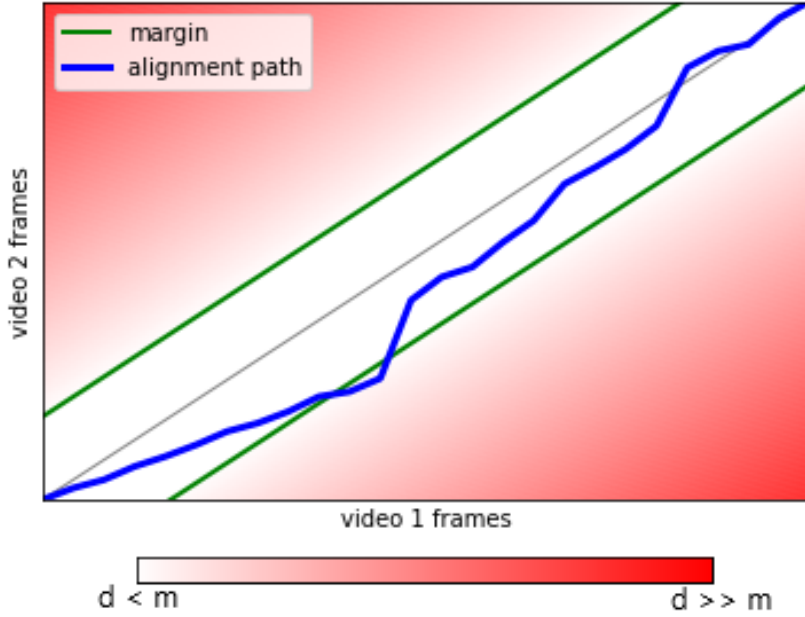


Fig. 4: DDTW method, the green lines parallel to the diagonal show the margin. The blue path shows the alignment of frames, and going out of the margin results in a penalty, which is calculated according to the distance from the diagonal.

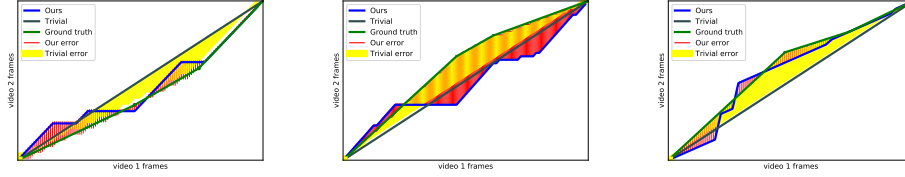


Fig. 5: The enclosed area for our predicted and trivial path for three pairs of videos. For the trivial method, the alignment path is the straight line passing through the lower left and upper right corners of the table.

2.4 Enclosed Area Error(EAE)

It is almost impossible to manually align two videos frame-by-frame in order to use them as ground truth. Therefore, in the literature, each video is divided into a number of phases, and metrics such as phase classification and correct phase rate are used to evaluate the alignment output. However, the problem with such metrics is that there is no ground truth alignment between frames, and these metrics are only based on the number of individual frames that are aligned to a frame from the correct phase of the other video. In this section, a new metric for the alignment of two videos, or generally two sequences that consist of a number of phases, is introduced. During each phase, it is natural to suppose that the process is going forward linearly, which is a rather correct assumption for the Penn action dataset(Zhang et al, 2013) and generally for human-action video datasets. By this assumption and knowing the boundaries of the phases in each video, a ground truth for the alignment can be obtained. We know some points on the ground truth path, and by the linearity assumption, the ground truth would be a piecewise-linear path going through those points(Figure 6). The metric, which measures the deviation from the ground truth, then equals the area between the ground truth and alignment path divided by the whole area of the rectangle.

3 Results

3.1 Dataset

The performance of our video alignment technique is evaluated on the Penn action dataset(Zhang et al, 2013). This dataset provides a collection of actions performed by different people with different variations. Also, to compare the performance of our technique with other methods, we used the phase labels prepared by the authors of Haresh et al (2021a) for this dataset. The complete list of all actions with the number of phases is given in Table 1

3.2 Baselines

For the experiments, in addition to using our proposed alignment method to align the videos, four other state-of-the-art methods are also implemented and used: GTA(Hadji et al, 2021a), TCC(Dwibedi et al, 2019), TCN(Sermanet et al, 2018), and SAL(Misra

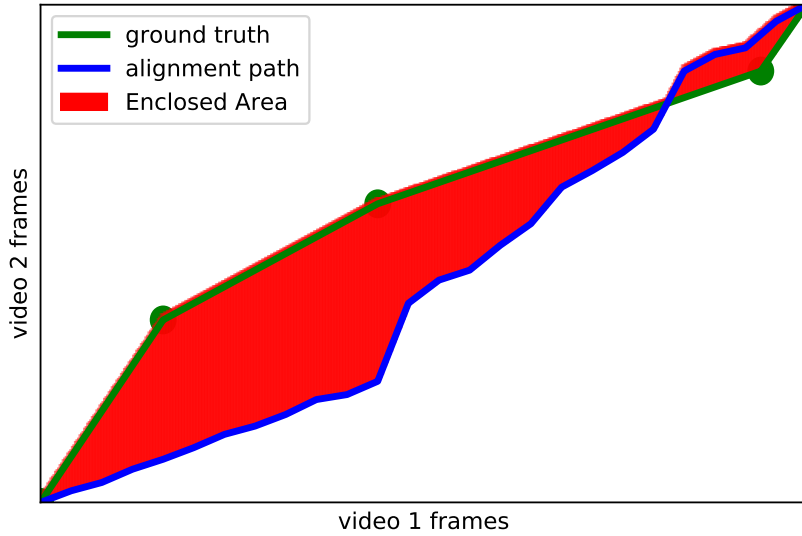


Fig. 6: Enclosed area is the area between ground truth and predicted path. The EAE metric computes what fraction of the table’s area is within the enclosed area.

et al, 2016). Moreover, a trivial baseline that aligns the frames of two videos linearly only based on their length is developed. This trivial method achieves outstanding results on the videos of this dataset because they have been trimmed, and extra/idle frames have been removed from them. An experiment is designed using synthesized videos that are closer to real-world videos to show the failure of the trivial method. The goal of this experiment is to show that the good performance of the trivial method on this dataset is by chance which is because of the special conditions of its videos. However, as it will be shown, our method is robust against various conditions.

SAL(Misra et al, 2016): This self-supervised method trains the Siamese network based on three-frame tuples and a classifier. The method randomly samples tuples from temporal windows with high motion and assigns positive or negative labels to them. This means that if the frames are in order, the tuple is considered positive, and if they are not in order, the tuple is considered negative. Additionally, the method trains the Classifier to predict whether the tuples are positive or negative.

TCN(Sermanet et al, 2018): In this work, a self-supervised method is introduced, involving a network trained on negative and positive frames. This method samples positives within a small window around anchors, while negatives are selected from distant timesteps within the same sequence. Additionally, the utilization of triplet loss in this work facilitates bringing anchors and positive frames closer to each other in the feature space compared to negative frames.

Table 1: Number of phases for each activity in Penn action dataset.

Action	Number of Phases
Baseball Pitch	4
Baseball Swing	3
Bench Press	2
Bowling	3
Clean and Jerk	6
Golf Swing	3
Jumping Jacks	4
Pullups	2
Pushups	2
Situps	2
Squats	4
Tennis Forehand	3
Tennis Serve	4

TCC([Dwibedi et al, 2019](#)): This self-supervised representation learning method trains a network using temporal cycle-consistency, which is a differentiable cycle-consistency loss that can find matched frames between two videos. This method produces per-frame embeddings for both videos and then uses Euclidian distance to align the frames of the second video to those of the first video.

GTA([Hadji et al, 2021a](#)): In this work, a weakly-supervised representation learning method trains a network based on a loss that is composed of two parts. The first part consists of alignment losses, that are based on cumulative sum computations along optimal respective paths. These losses focus on achieving a consistent temporal alignment between frames of different videos. The second part of the loss involves global cycle consistency, utilized to ensure the stability of learned representations through cycle consistency.

Trivial: This method aligns two videos only based on their numbers of frames, using an assumption that in all videos, the process is going forward linearly. It means that if the first and second videos have n and m frames, respectively, then the $i - th$ frame of the first video is aligned to the $\frac{i}{n} \times j - th$ frame of the second video. Figure 5 shows EAE for trivial and our method on three pairs of videos.

3.3 Metrics

In this work, three evaluation metrics are used: EAE, correct phase rate, and phase classification accuracy. EAE, which is our proposed metric, is explained in Section 2.3. This metric evaluates video synchronization task.

Correct Phase Rate([Becattini et al, 2020](#); [Heidarivincheh et al, 2018](#)): This metric finds the portion of the frames in the reference video that are aligned to any frame in the correct phase in the second video. This metric, which evaluates the video synchronization task, is calculated after frame alignment.

Phase classification accuracy: This is the per frame phase classification accuracy on test data. To perform phase classification, an SVM is trained using the phase labels for each frame of the videos. Also, in this work, to ensure a fair comparison

between the methods, care is taken to prevent overlap between the training data used for the feature extraction (in self-supervised methods) and the data used for SVM training. During the evaluation phase, a 10-fold cross-validation is employed. In each iteration, one part of the test data is used as the training set for SVM, and the remaining data is reserved for testing purposes. This robust methodology is used for more accurate evaluation of the proposed method.

3.4 Results

The proposed method is evaluated using two tasks: phase classification and video synchronization.

3.4.1 Phase Classification

Our final features are evaluated on the phase classification task and compared with the performance of SAL(Misra et al, 2016), TCN(Sermanet et al, 2018), TCC(Dwibedi et al, 2019) and GTA(Hadji et al, 2021a) methods. In this setting, 10-fold cross-validation is used on the test data. As shown in Table 2, our method significantly outperforms the other methods in this task, demonstrating the effectiveness of the proposed features. However, it is noteworthy that in the Bench Press, Pushup, and Situp actions, the TCC(Dwibedi et al, 2019) and GTA(Hadji et al, 2021a) results are higher than those achieved by our method. This difference could potentially be attributed to a specific positioning of the main subject during these actions, leading to errors in the pose estimation process and consequently in the features based on pose estimation. It is worth mentioning that video alignment is not performed during this experiment, and only the effectiveness of the extracted features is evaluated.

Table 2: Phase Classification Accuracy(%) on different activities in Penn action dataset.

	SAL	TCN	TCC	GTA	Ours
Type of feature extraction	self-supervised	self-supervised	self-supervised	weakly-supervised	unsupervised
Baseball Pitch	45	42	68	81	87
Baseball Swing	52	48	66	85	84
Bench Press	49	55	76	88	65
Bowling	49	64	64	75	76
Clean and Jerk	46	38	65	73	78
Golf Swing	55	71	69	83	91
Jumping Jacks	34	64	66	82	86
Pullups	52	53	77	53	85
Pushups	46	85	74	87	74
Situps	54	61	81	52	78
Squats	42	72	74	82	82
Tennis Forehand	57	57	63	73	82
Tennis Serve	39	47	62	75	84
Overall	47.69	58.2	69.6	76.3	80.92

Table 3: Correct phase rate and E/AE results on different activities in Penn action dataset.

	SAL	Correct phase rate(%)						E/AE					
		TCN	TCC	GTA	Trivial	Ours	SAL	TCN	TCC	GTA	Trivial	Ours	
Baseball Pitch	67	66	65	71	69	82	0.107	0.117	0.123	0.1	0.079	0.054	
Baseball Swing	67	74	68	79	81	79	0.158	0.098	0.155	0.101	0.055	0.079	
Bench Press	77	81	81	87	88	84	0.161	0.138	0.138	0.094	0.06	0.102	
Bowling	65	71	64	70	75	77	0.161	0.116	0.162	0.127	0.084	0.089	
Clean and Jerk	43	58	51	60	68	81	0.2	0.126	0.145	0.122	0.056	0.049	
Golf Swing	72	80	77	84	88	90	0.14	0.079	0.105	0.069	0.034	0.038	
Jumping Jacks	66	75	73	85	85	87	0.111	0.068	0.075	0.042	0.032	0.031	
Pullups	79	84	82	80	91	90	0.157	0.107	0.126	0.146	0.042	0.065	
Pushups	80	83	81	90	91	87	0.146	0.122	0.133	0.075	0.043	0.081	
Situps	80	86	85	87	73	88	0.145	0.102	0.106	0.084	0.034	0.077	
Squats	60	69	71	77	76	78	0.173	0.113	0.096	0.074	0.055	0.061	
Tennis Forehand	72	79	69	73	83	86	0.139	0.092	0.151	0.132	0.051	0.062	
Tennis Serve	60	65	65	66	75	80	0.147	0.11	0.117	0.11	0.064	0.058	
Overall	68.3	74.7	71.7	77.6	81.8	83.8	0.15	0.107	0.125	0.098	0.053	0.065	

Table 4: The overall result of the experiment shows the inefficiency of the trivial method on the other types of data.

	EAE	Correct phase rate
Trivial	0.157	0.417
Ours	0.108	0.555

3.4.2 Video Synchronization

The results of video synchronization for the five methods are provided for each action in Table 3. Results show that our final method (feature vector extraction + DDTW) performs significantly better than the other state-of-the-art methods in the video alignment task.

An experiment is provided to show that the good results of the trivial method on the Penn dataset cannot be generalized to other datasets. The reason for the good performance of this method here is that the videos in the Penn action dataset are trimmed, i.e., idle frames are removed from the beginning and end of the videos. Also, there is no noticeable change in the speed of performing different phases of any action. In other words, the videos of the same action can be aligned with each other by linear expansion or shrinkage in the time domain. In this experiment, realistic modifications are applied to the videos to generate new ones for which the trivial method fails to align them successfully with the original videos. To this end, a "wait phase" is added at the beginning of all videos, by repeating the first three frames of the video; If the original video has n frames, then $\frac{n}{2}$ frames are added at the beginning to generate a new video with $\frac{3n}{2}$ frames. This modification is realistic because it is natural to wait and concentrate before starting an exercise. As it is shown in table 4, the trivial method fails to align modified videos to original ones effectively, and our method performs significantly better than trivial.

4 Conclusion

This paper presents an unsupervised method for aligning two videos with the same action but different execution and appearance. In this method, a video is modeled as a multi-dimensional time series containing global and local, and static and dynamic features of its frames. A modified DTW method is also introduced for aligning time series, and a new metric is presented to compare the performance of time series alignment methods effectively. The results show that the proposed method provides significant performance improvement compared to the other methods and can be implemented for any action performed by one subject without any need for training any network. This work adds to the field of video alignment and has the potential to improve various video-related tasks such as action recognition, anomaly detection, and tracking.

References

- Babu SC (2019) A 2019 guide to human pose estimation with deep learning. <https://nanonets.com/blog/human-pose-estimation-2d-guide/>
- Bar-Shalom G, Leifman G, Elad M, et al (2023) Weakly-supervised representation learning for video alignment and analysis. arXiv preprint arXiv:230204064
- Becattini F, Uricchio T, Seidenari L, et al (2020) Am i done? predicting action progress in videos. *ACM Transactions on Multimedia Computing, Communications, and Applications (TOMM)* 16(4):1–24
- Bojanowski P, Lajugie R, Grave E, et al (2015) Weakly-supervised alignment of video with text. In: *Proceedings of the IEEE international conference on computer vision*, pp 4462–4470
- Broström M (2020) Real-time multi-object tracker using yolov5 and deep sort. https://github.com/mikel-brostrom/Yolov5_DeepSort_Pytorch
- Cao K, Ji J, Cao Z, et al (2020) Few-shot video classification via temporal alignment. In: *Proceedings of the IEEE/CVF Conference on Computer Vision and Pattern Recognition*, pp 10618–10627
- Chai J, Zeng H, Li A, et al (2021) Deep learning in computer vision: A critical review of emerging techniques and application scenarios. *Machine Learning with Applications* 6:100134
- Chang CY, Huang DA, Sui Y, et al (2019) D3tw: Discriminative differentiable dynamic time warping for weakly supervised action alignment and segmentation. In: *Proceedings of the IEEE/CVF Conference on Computer Vision and Pattern Recognition*, pp 3546–3555
- Chung JL, Ong LY, Leow MC (2022) Comparative analysis of skeleton-based human pose estimation. *Future Internet* 14(12):380
- Deng J, Dong W, Socher R, et al (2009) Imagenet: A large-scale hierarchical image database. In: *2009 IEEE conference on computer vision and pattern recognition*, Ieee, pp 248–255
- Dwibedi D, Aytar Y, Tompson J, et al (2019) Temporal cycle-consistency learning. In: *Proceedings of the IEEE/CVF conference on computer vision and pattern recognition*, pp 1801–1810
- Elharrouss O, Akbari Y, Almaadeed N, et al (2022) Backbones-review: Feature extraction networks for deep learning and deep reinforcement learning approaches. arXiv preprint arXiv:220608016

- Fernando B, Shirazi S, Gould S (2017) Unsupervised human action detection by action matching. In: Proceedings of the IEEE Conference on Computer Vision and Pattern Recognition Workshops, pp 1–9
- Hadji I, Derpanis KG, Jepson AD (2021a) Representation learning via global temporal alignment and cycle-consistency. In: Proceedings of the IEEE/CVF Conference on Computer Vision and Pattern Recognition, pp 11068–11077
- Hadji I, Derpanis KG, Jepson AD (2021b) Representation learning via global temporal alignment and cycle-consistency. In: Proceedings of the IEEE/CVF Conference on Computer Vision and Pattern Recognition, pp 11068–11077
- Hareh S, Kumar S, Coskun H, et al (2021a) Learning by aligning videos in time. In: Proceedings of the IEEE/CVF Conference on Computer Vision and Pattern Recognition, pp 5548–5558
- Hareh S, Kumar S, Coskun H, et al (2021b) Learning by aligning videos in time. In: Proceedings of the IEEE/CVF Conference on Computer Vision and Pattern Recognition, pp 5548–5558
- Heidarvinchek F, Mirmehdi M, Damen D (2018) Action completion: A temporal model for moment detection. arXiv preprint arXiv:180506749
- Kumar G, Bhatia PK (2014) A detailed review of feature extraction in image processing systems. In: 2014 Fourth international conference on advanced computing & communication technologies, IEEE, pp 5–12
- Li S, Liu H, Qian R, et al (2022) Ta2n: Two-stage action alignment network for few-shot action recognition. In: Proceedings of the AAAI Conference on Artificial Intelligence, pp 1404–1411
- Liu J, Shi M, Chen Q, et al (2021) Normalized human pose features for human action video alignment. In: Proceedings of the IEEE/CVF International Conference on Computer Vision, pp 11521–11531
- Liu W, Tekin B, Coskun H, et al (2022) Learning to align sequential actions in the wild. In: Proceedings of the IEEE/CVF Conference on Computer Vision and Pattern Recognition, pp 2181–2191
- Lu C, Mandal M (2010) Efficient temporal alignment of video sequences using unbiased bidirectional dynamic time warping. *Journal of Electronic Imaging* 19(4):040501–040501
- Misra I, Zitnick CL, Hebert M (2016) Shuffle and learn: unsupervised learning using temporal order verification. In: Computer Vision—ECCV 2016: 14th European Conference, Amsterdam, The Netherlands, October 11–14, 2016, Proceedings, Part I 14, Springer, pp 527–544

- Müller M (2007) Information retrieval for music and motion, vol 2. Springer
- Munea TL, Jembre YZ, Weldegebriel HT, et al (2020) The progress of human pose estimation: A survey and taxonomy of models applied in 2d human pose estimation. *IEEE Access* 8:133330–133348
- Prätzlich T, Driedger J, Müller M (2016) Memory-restricted multiscale dynamic time warping. In: 2016 IEEE International Conference on Acoustics, Speech and Signal Processing (ICASSP), IEEE, pp 569–573
- Purushwalkam S, Ye T, Gupta S, et al (2020) Aligning videos in space and time. In: *Computer Vision–ECCV 2020: 16th European Conference, Glasgow, UK, August 23–28, 2020, Proceedings, Part XXVI* 16, Springer, pp 262–278
- Sakoe H, Chiba S (1978) Dynamic programming algorithm optimization for spoken word recognition. *IEEE transactions on acoustics, speech, and signal processing* 26(1):43–49
- Sáráandi I, Linder T, Arras KO, et al (2021) MeTRAbs: metric-scale truncation-robust heatmaps for absolute 3D human pose estimation. *IEEE Transactions on Biometrics, Behavior, and Identity Science* 3(1):16–30. <https://doi.org/10.1109/TBIOM.2020.3037257>
- Sermanet P, Lynch C, Chebotar Y, et al (2018) Time-contrastive networks: Self-supervised learning from video. In: 2018 IEEE international conference on robotics and automation (ICRA), IEEE, pp 1134–1141
- Simonyan K, Zisserman A (2014) Very deep convolutional networks for large-scale image recognition. *arXiv preprint arXiv:14091556*
- Song YC, Naim I, Al Mamun A, et al (2016) Unsupervised alignment of actions in video with text descriptions. In: *IJCAI*, pp 2025–2031
- Wang J, Long Y, Pagnucco M, et al (2021) Dynamic graph warping transformer for video alignment. *British Machine Vision Conference*
- Wojke N, Bewley A, Paulus D (2017) Simple online and realtime tracking with a deep association metric. In: 2017 IEEE international conference on image processing (ICIP), IEEE, pp 3645–3649
- Zhang Q, Xiao T, Efros AA, et al (2020) Learning cross-domain correspondence for control with dynamics cycle-consistency. *arXiv preprint arXiv:201209811*
- Zhang S, Zhou J, He X (2021) Learning implicit temporal alignment for few-shot video classification. *arXiv preprint arXiv:210504823*
- Zhang W, Zhu M, Derpanis KG (2013) From actemes to action: A strongly-supervised representation for detailed action understanding. In: *Proceedings of the IEEE*

international conference on computer vision, pp 2248–2255

Zhao Y, Li Z, Guo X, et al (2022) Alignment-guided temporal attention for video action recognition. arXiv preprint arXiv:221000132

Zhou F, Torre F (2009) Canonical time warping for alignment of human behavior. Advances in neural information processing systems 22